Supplementary Materials

Influence of SPIONs Surface Coating on Magnetic Properties and Theranostic Profile

Vital Ferreira-Filho [1], Beatriz Morais [1], Bruno J. C. Vieira [1], João Carlos Waerenborgh [1], Maria J. Carmezim [2,3], Csilla Noémi Tóth [4], Sandra Même [4], Sara Lacerda [4], Daniel Jaque [5], Célia T. Sousa [6], Maria Paula Cabral Campello [1,*] and Laura C. J. Pereira [1,*]

[1] Centro de Ciências e Tecnologias Nucleares, DECN, Instituto Superior Técnico, Universidade de Lisboa, E.N. 10, km 139,7, 2695-066 Bobadela LRS, Portugal; vital.filho@ctn.tecnico.ulisboa.pt (VFF); beatriz.morais@ctn.tecnico.ulisboa (BM); ptbrunovieira@ctn.tecnico.ulisboa.pt (B.J.C.V.); jcarlos@ctn.tecnico.ulisboa.pt (J.C.W.); pcampelo@ctn.tecnico.ulisboa.pt (MPCC); lpereira@ctn.tecnico.ulisboa.pt (L.C.J.P.).

[2] Centro de Química Estrutural-CQE, DEQ, Instituto Superior Técnico, Universidade de Lisboa, Av. Rovisco Pais, 1049-001 Lisboa, Portugal; maria.carmezim@estsetubal.ips.pt (MJC).

[3] ESTSetúbal, CDP2T, Instituto Politécnico de Setúbal, Setúbal, Portugal; maria.carmezim@estsetubal.ips.pt (MJC).

[4] Centre de Biophysique Moléculaire, CNRS, UPR 4301, Université d'Orléans, Rue Charles Sadron,45071 Orléans CEDEX 2, France; csilla.gardatoht@cnrs-orleans.fr (CGT); sandra.meme@cnrs-orleans.fr (SM); sara.lacerda@cnrs-orleans.fr (SL).

[5] Departamento de Física de Materiales, Universidad Autonoma de Madrid, Avda. Francisco Tomás y Valiente 7, 28049 Madrid, Spain; daniel.jaque@uam.es (DJ).

[6] Departamento de Física Aplicada, Universidad Autonoma de Madrid, Avda. Francisco Tomás y Valiente 7, 28049 Madrid, Spain; celia.tsousa@uam.es (CTS).

* Correspondence: pcampelo@ctn.tecnico.ulisboa.pt (MPCC); lpereira@ctn.tecnico.ulisboa.pt (L.C.J.P.).; Tel.: +351219946233 (MPCC); Tel.:+ 351219946259 (LCJP).

Contents **Page**

1. *UV-Vis Spectrophotometry*

Table S1. Absorption peaks observed in the UV-Vis Spectra of the SPIONs

Sample	Wavelength (nm)	
$SP_{R/P}$	244	326
$SP_{R/P}$-Dx	248	388
$SP_{R/P}$-Dx-Au	390	543
$SP_{R/P}$-Dx-Au-Gd	394	544
SP_{pH}	251	320
SP_{pH}-Dx	229	381
SP_{pH}-Dx-Au	385	530
SP_{pH}-Dx-Au-Gd	395	540
Dextran	275	

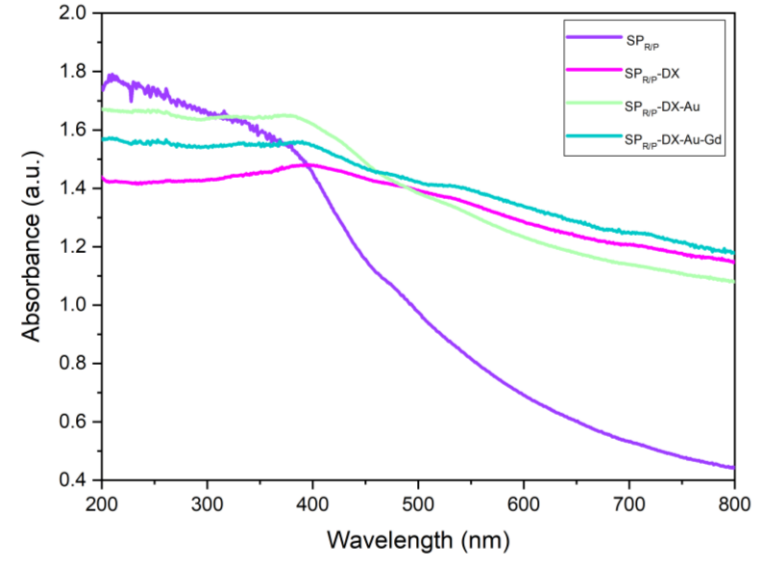

Figure S1. UV-Vis spectra of SPR/P SPIONs

2. *Attenuated Total Reflectance Fourier-Transform Infrared Spectroscopy (ATR-FTIR)*

Table S2. Most Significant absorption bands observed in the FTIR Spectra of the SPIONs

Sample	**Wavenumber (cm^{-1})**								
$SP_{R/P}$	3445	2920	2849	2360	1635	1384			419
$SP_{R/P}$-Dx	3420	2923	2853	2360	1636		1152	1015	576
$SP_{R/P}$-Dx-Au	3446	2918	2849	2360	1646	1463	1111	1015	577
$SP_{R/P}$-Dx-Au-Gd	3420	2922	2843	2359	1646	1457	1157	1017	586
SP_{pH}	3423	3134			1634	1384	1114	863	588
SP_{pH}-Dx	3422	2923			1636	1384	1110	1016	579
SP_{pH}-Dx-Au	3422	2923			1647	1384	1110	1013	581
SP_{pH}-Dx-Au-Gd	3419	3196	2922	2851	1634	1384	1111		590

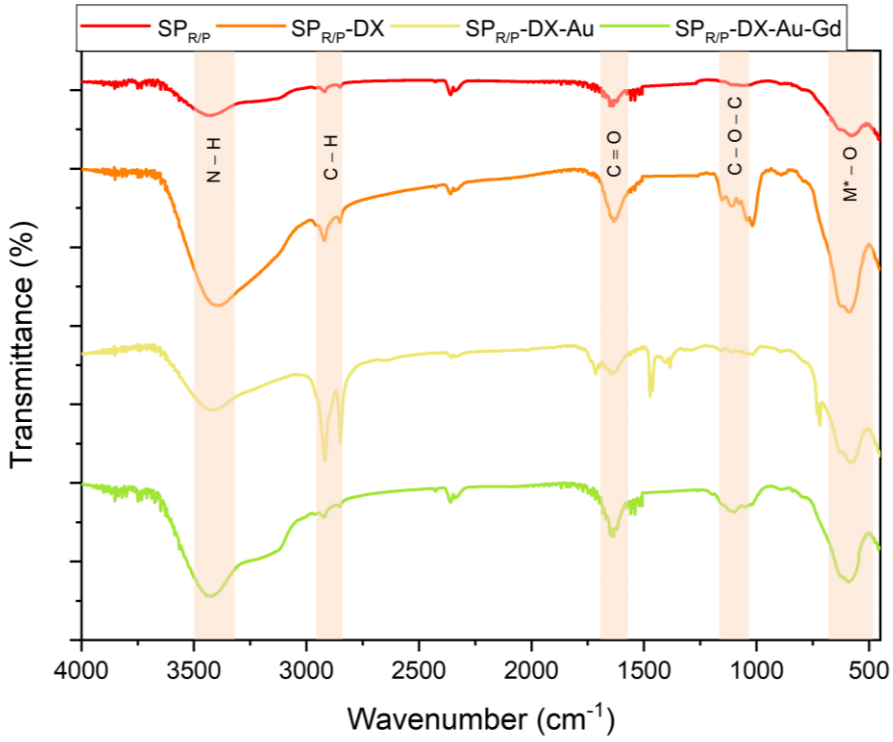

Figure S2. ATR-FTIR spectra of $SP_{R/P}$-based nanoplatforms.

3. *Powder X-ray diffraction (PXRD)*

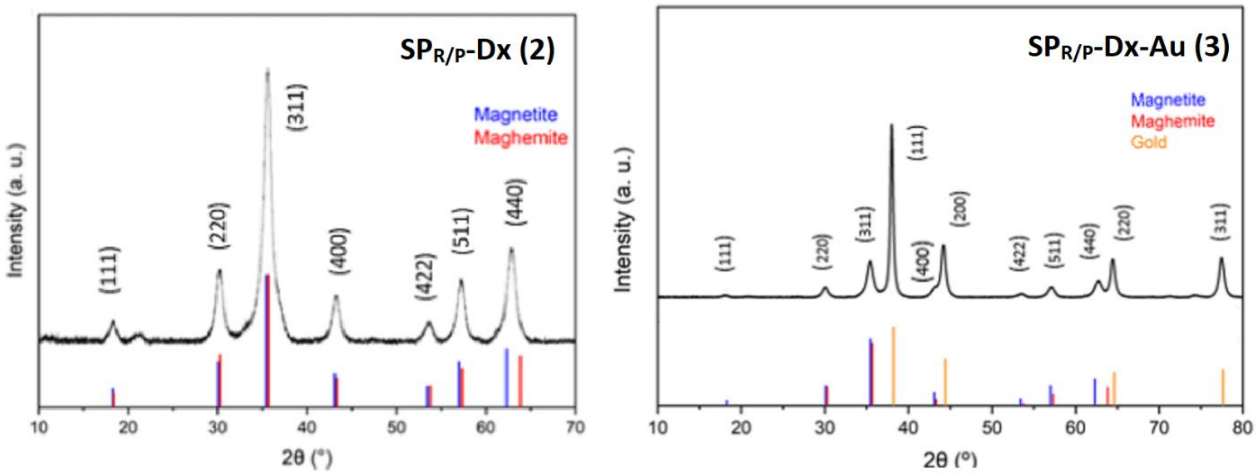

Figure S3. Powder diffractogram of coated samples **2** (left) and **3** (right).

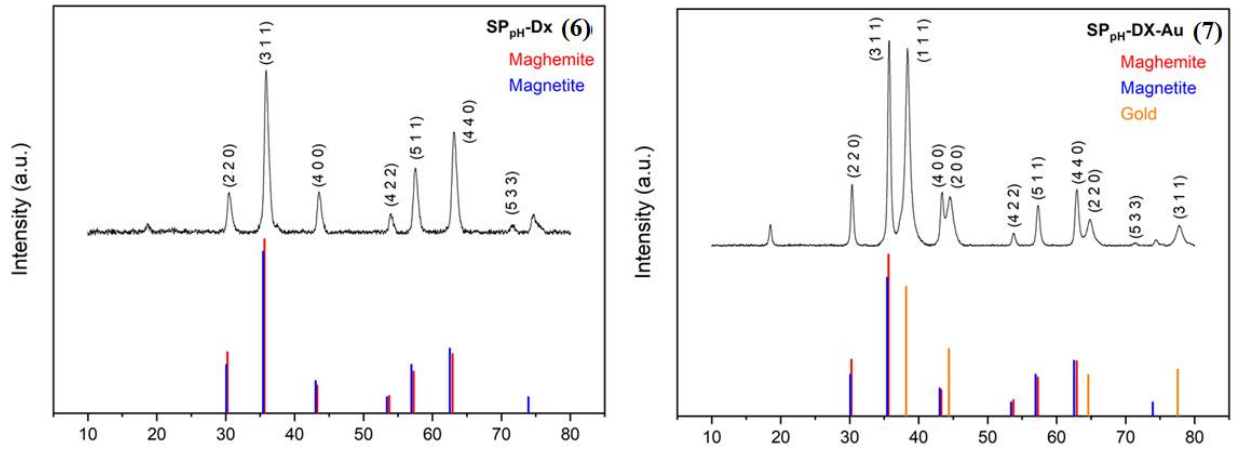

Figure S4. Powder diffractogram of coated samples **6** (left) and **7** (right).

4. *Transmission Electron Microscopy (TEM)*

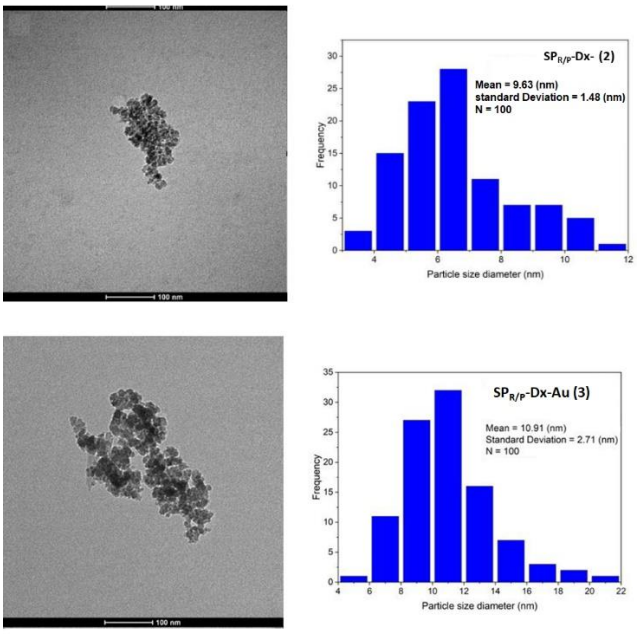

Figure S5. Transmission electron microscopy images of the SPIONs respective size histogram: Top: SP$_{R/P}$-Dx (**2**); bottom: SP$_{R/P}$-Dx-Au (**3**).

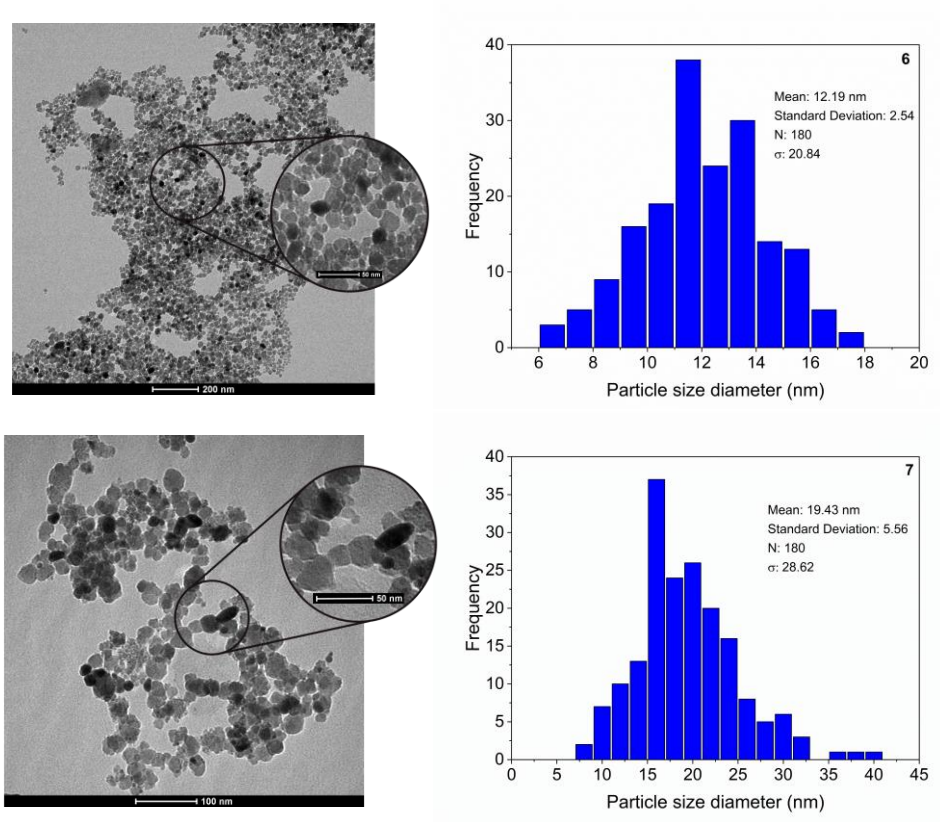

Figure S6. Transmission electron microscopy images of the SPIONs respective size histogram: Top: SP$_{pH}$-Dx (**6**); bottom: SP$_{pH}$-Dx-Au (**7**).

5. *Mössbauer Spectroscopy*

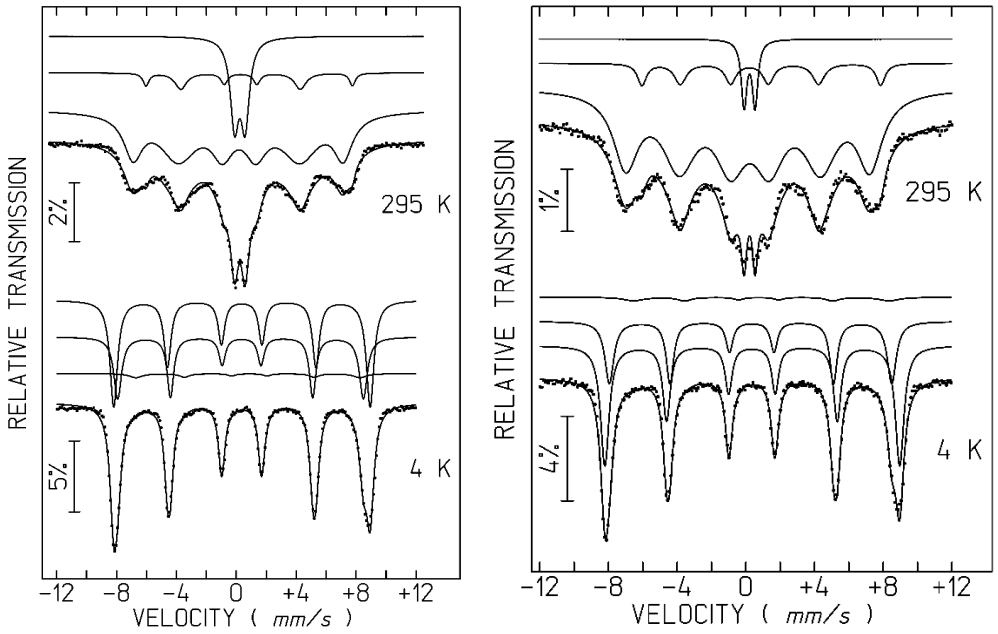

Figure S7. Mössbauer spectra of $SP_{R/P}$ (left) and $SP_{R/P}$-Dx-Au (right) taken at different temperatures. The lines over the experimental points are the calculated curves. The estimated parameters are collected in Table S3.

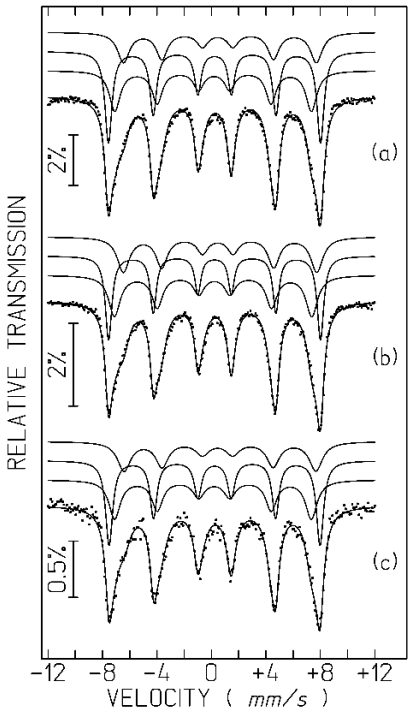

Figure S8. Room temperature Mössbauer spectra of (a) SP_{pH}-Dx (b) SP_{pH}-Dx-Au and (c) SP_{pH}-Dx-Au-Gd samples. Calculated lines on the experimental points are the sum of three sextets (see Table S3).

Table S3. Estimated parameters from the Mössbauer spectra of selected SPIONs samples at room temperature and at 4 K.

Sample	IS mm/s	ε mm/s	B_{hf} tesla	I (%)	Fe state	Fe in Fe_3O_4
$SP_{R/P}$ (1)	0.30	-0.12	43.5	76%	Fe^{3+} γFe_2O_3 , Fe_3O_4	**11%**
295 K	0.35	0.65	-	16%	Fe^{3+} in the smallest NPs	
	0.69	0.66	42.7	8%	$Fe^{2.5+}$ CN = 6 Fe_3O_4	
4 K	0.43	-0.07	50.9	39%	Fe^{3+} CN=4 γFe_2O_3 , Fe_3O_4	
	048	0.02	53.1	57%	Fe^{3+} CN = 6 γFe_2O_3 , Fe_3O_4	
	0.93	-0.10	46.4	3.8%	Fe^{2+} CN = 6 Fe_3O_4	
$SP_{R/P}$-Dx (2)	0.29	-0.09	43.4	75%	Fe^{3+} γFe_2O_3 , Fe_3O_4	**11%**
295 K	0.35	0.69	-	17%	Fe^{3+} in the smallest NPs	
	0.68	0.63	42.1	8%	$Fe^{2.5+}$ CN = 6 Fe_3O_4	
4 K	0.42	-0.08	50.9	38%	Fe^{3+} CN=4 γFe_2O_3 , Fe_3O_4	
	048	0.01	53.0	58%	Fe^{3+} CN = 6 γFe_2O_3 , Fe_3O_4	
	0.93	-0.45	46.8	3.8%	Fe^{2+} CN = 6 Fe_3O_4	
$SP_{R/P}$-Dx-Au (3)	0.29	-0.12	44.1	86%	Fe^{3+} γFe_2O_3 , Fe_3O_4	**13%**
295 K	0.33	0.64	-	5%	Fe^{3+} in the smallest NPs	
	0.67	0.69	43.1	9%	$Fe^{2.5+}$ CN = 6 Fe_3O_4	
4 K	0.43	-0.07	51.0	38%	Fe^{3+} CN=4 γFe_2O_3 , Fe_3O_4	
	048	0.02	53.3	58%	Fe^{3+} CN = 6 γFe_2O_3 , Fe_3O_4	
	0.94	0.23	46.5	4.4%	Fe^{2+} CN = 6 Fe_3O_4	
SP_{pH} (5)	0.26	-0.09	44.3	32%	Fe^{3+} CN=4 γFe_2O_3 , Fe_3O_4	**33%**
295 K	0.33	0.01	48.6	47%	Fe^{3+} CN = 6 γFe_2O_3	
	0.66	0.26	42.8	21%	$Fe^{2.5+}$ CN = 6 Fe_3O_4	
4 K	0.43	0.00	51.6	34%	Fe^{3+} CN=4 γFe_2O_3 , Fe_3O_4	
	0.51	-0.03	53.6	56%	Fe^{3+} CN = 6 γFe_2O_3 , Fe_3O_4	
	0.94	-0.31	46.9	11%	Fe^{2+} CN = 6 Fe_3O_4	

SP_{pH}-Dx (6)	0.27	-0.08	44.8	31	Fe^{3+} CN=4 γFe_2O_3 , Fe_3O_4	**39%**
295 K	0.34	-0.01	48.3	43	Fe^{3+} CN = 6 γFe_2O_3	
	0.65	0.17	43.9	26	$Fe^{2.5+}$ CN = 6 Fe_3O_4	
SP_{pH}-Dx-Au (7)	0.28	-0.10	44.7	33	Fe^{3+} CN=4 γFe_2O_3 , Fe_3O_4	**45%**
295 K	0.34	-0.01	48.3	37	Fe^{3+} CN = 6 γFe_2O_3	
	0.66	0.17	44.1	30	$Fe^{2.5+}$ CN = 6 Fe_3O_4	
SP_{pH}-Dx-Au-Gd (8)	0.27	-0.10	45.0	34	Fe^{3+} CN=4 γFe_2O_3 , Fe_3O_4	**44%**
295 K	0.34	0.00	48.1	37	Fe^{3+} CN = 6 γFe_2O_3	
	0.65	**0.19**	**43.9**	**29**	**$Fe^{2.5+}$ CN = 6 Fe_3O_4**	

IS isomer shift relative to metallic α-Fe at 298 K; $\varepsilon = (e^2QV_{zz}/4)(3\cos^2\theta - 1)$ quadrupole shift, B_{hf} magnetic hyperfine field. I relative area. CN coordination number. Estimated errors ≤ 0.02 mm/s for IS, ε, Γ, < 0.3 T for B_{hf} and < 2% for I.

6. *Magnetization Measurements*

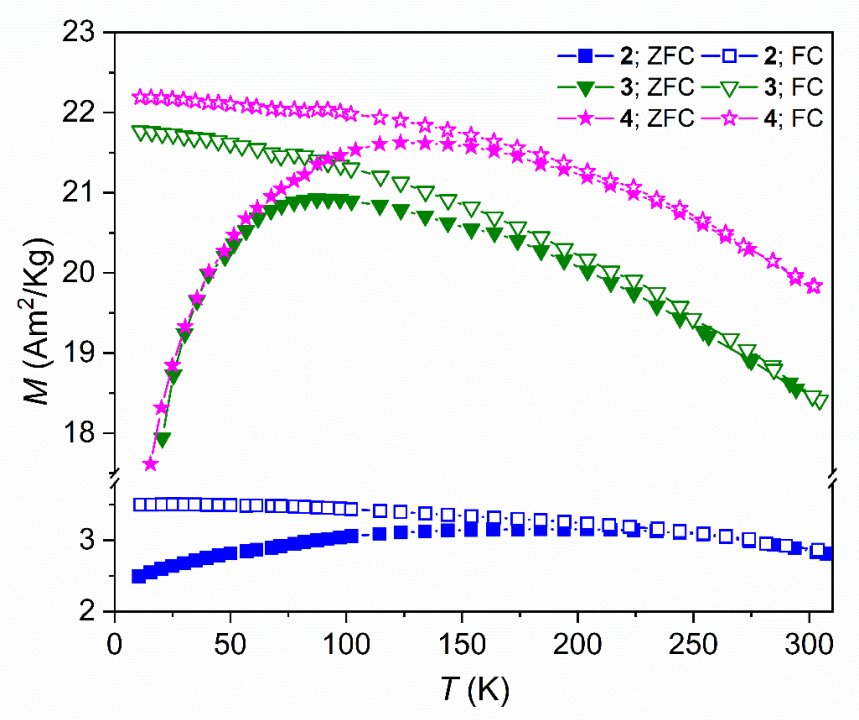

Figure S9. Temperature dependence of the zero-field cooling (ZFC) and field cooling (FC) magnetization for $SP_{R/P}$-based samples, **2** (at 10mT) **3** and **4** (at 50 mT).

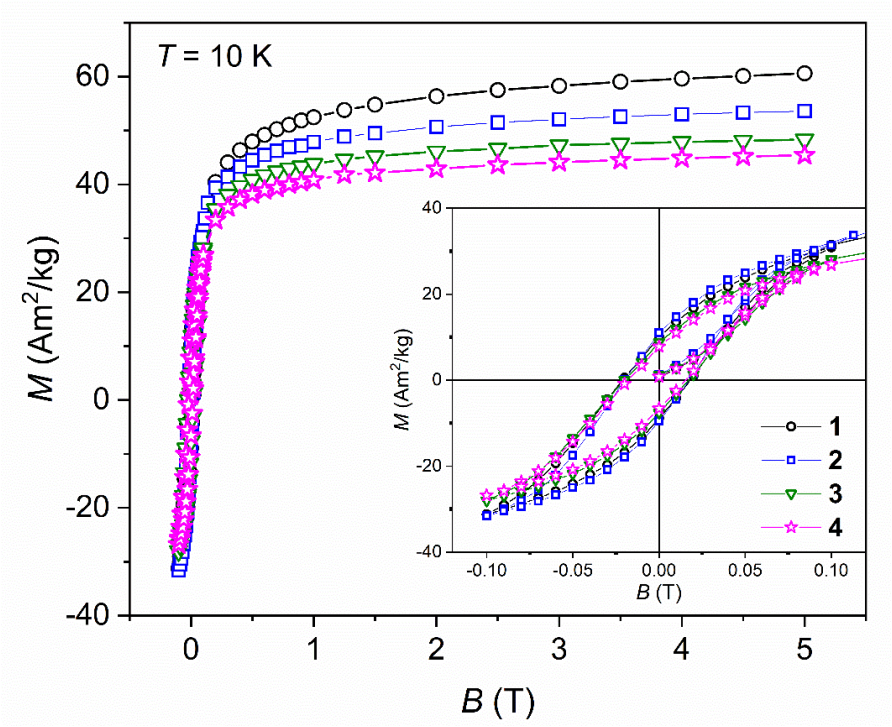

Figure S10. Magnetic field (*B*) dependence of magnetization (*M*) at 10 K for $SP_{R/P}$-based samples **1** to **4.**

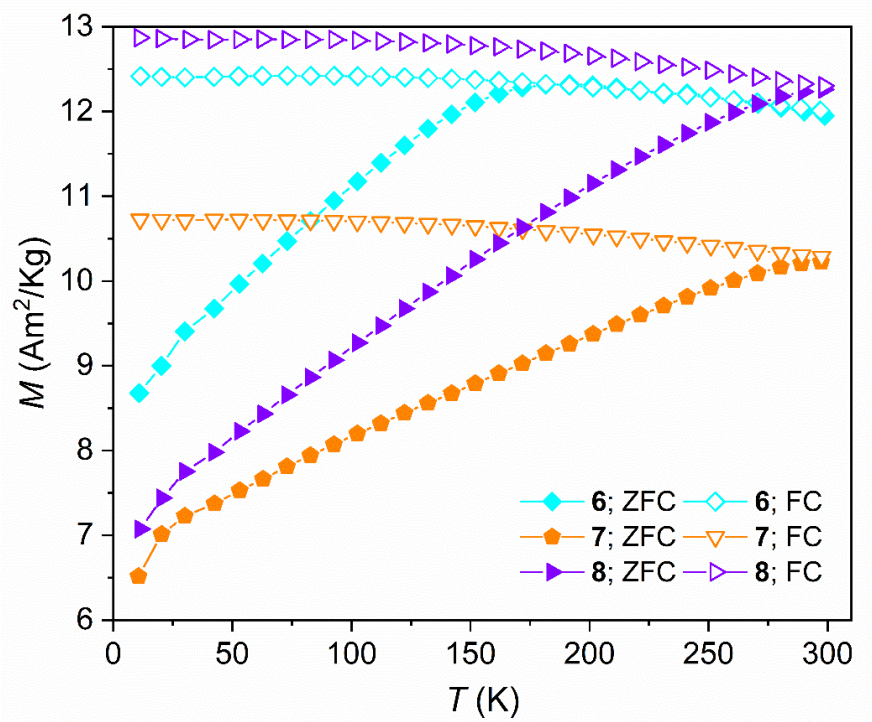

Figure S11. Temperature dependence of the zero-field cooling (ZFC) and field cooling (FC) magnetization for SP_{pH}-based samples, **6**, **7**, **8** (at 10 mT).

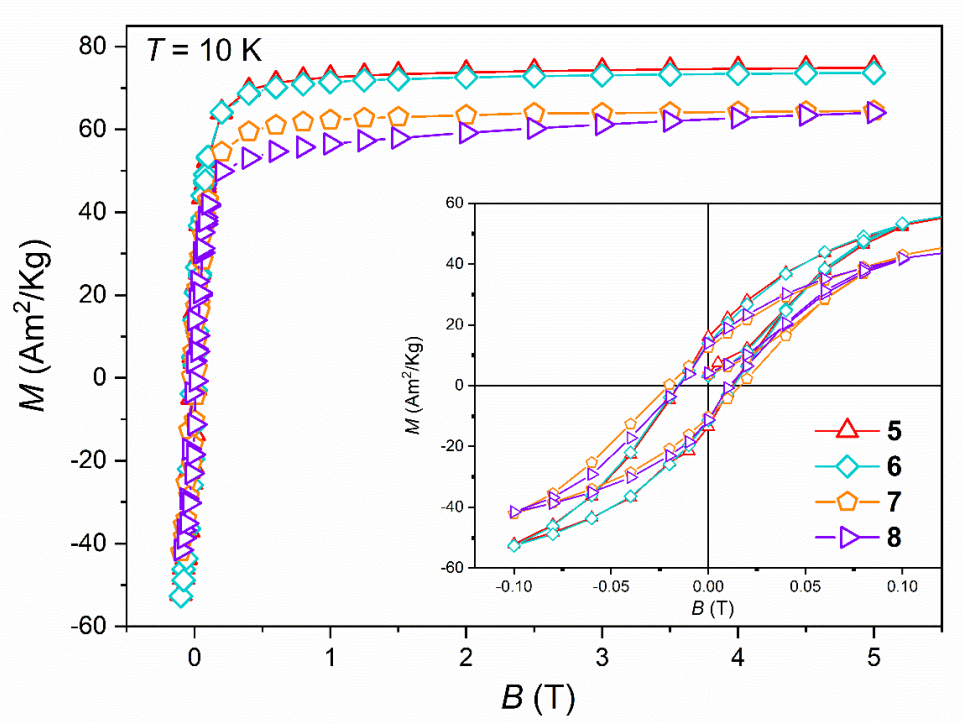

Figure S12. Magnetic field (*B*) dependence of magnetization (*M*) at 10 K for SP_{pH}-based samples **5** to **8.**